Sophi Shilpa Gururajapathy[1], Hazlie Mokhlis[1,*], HazleeAzil Illias[1], AbHalim Abu Bakar[2] , LilikJamilatul Awalin[3]

J. Electrical Systems 12-4 (2016): 786-800

Regular paper

Fault Identification in an Unbalanced Distribution System Using Support Vector Machine

Fast and effective fault location in distribution system is important to improve the power system reliability. Most of the researches rarely mention about effective fault location consisting of faulted phase, fault type, faulty section and fault distance identification. This work presents a method using support vector machine to identify the faulted phase, fault type, faulty section and distance at the same time. Support vector classification and regression analysis are performed to locate fault. The method uses the voltage sag data during fault condition measured at the primary substation. The faulted phase and the fault type are identified using three-dimensional support vector classification. The possible faulty sections are identified by matching voltage sag at fault condition to the voltage sag in database and the possible sections are ranked using shortest distance principle. The fault distance for the possible faulty sections isthen identified using support vector regression analysis. The performance of the proposed method was tested on an unbalanced distribution system from SaskPower, Canada. The results show that the accuracy of the proposed method is satisfactory.

Keywords: Support Vector Machine; Faulted Phase; Fault type; Faulty section; Fault distance.

Article history: Received 8 June 2016, Accepted 25 October 2016

1. Introduction

Distribution systems supply electric power to customers and occupy an important role in power system. A survey in [1] shows that more than 80% of the interruption in distribution systems was caused by faults, which damaged the equipment and led to power outage to every customer on the system. This situation has forced electrical power utilities to provide high reliable and quality power supply [2]. Hence, to maintain continuous power supply to customers, faulty line has to be identified and isolated from the system. An effective fault location identification in distribution systems should be able to identify the faulted phase, fault type, faulty section and fault distance. Identification of faulted phase, fault type and faulty section further helps to know the most frequent type of fault occurred in particular system. Thus,proper maintenance can be taken to minimize its occurrence in the future.

Various knowledge based algorithms have been used to identify fault such as the Artificial Neural Network (ANN) [3], Wavelet Transform (WT), Fuzzy Theory, Matching approach and Support Vector Machine (SVM). The method using voltage sag characteristic [4, 5] identifies the fault type by comparing the pattern of pre-fault voltage with the voltage during fault. However, for fault far from the measurement location, the different is not

* Corresponding author: H. Mokhlis, Department of Electrical Engineering, Faculty of Engineering, University of Malaya, 50603 Kuala Lumpur, Malaysia, E-mail: hazli@um.edu.my

[1]Department of Electrical Engineering, Faculty of Engineering, University of Malaya, 50603 Kuala Lumpur, Malaysia

[2]UM Power Energy Dedicated Advanced Centre (UMPEDAC) Level 4, Wisma R&D, University of Malaya, JalanPantaiBaru, 59990 Kuala Lumpur, Malaysia

[3]University Kuala Lumpur, Electrical Engineering Section, International College, British Malaysian Institute, Batu 8, Jalan Sungai Pusu, 53100,Gombak, Selangor, Malaysia

noticeable and may lead to wrong identification of fault type. Fuzzy set wasproposed in [6-8] and neural network in [9] for fault type classification.The methods such as in [10, 11] identify fault type for transmission systems using SVM. The method in [10] uses zero sequence and three phase currents to identify the faulted phase in transmission system. In [11], fault classification using principal component analysis and SVM is proposed.

SVM wasused for faultclassification and sectionidentification in [12]. ANN wasproposed in [13], which uses voltage and current to classify Double Line to Ground Fault. The method in [13]identifiedthe fault type and faulty section. A combination of SVM and Wavelet transform was proposed in [14] for prediction of fault type and location. It uses voltage and current signals to locate fault in transmission system. Fault location with WT and wavelet packet transform (WPT) combining artificial neural network was proposed in [15]. A hybrid approach using wavelet transform and SVM was suggested in [16] for precise fault location in transmission lines. A method to identify faulty section and fault distance by using matching approach was proposed in [17, 18]. The method in [18] also ranks the possible section based on priority. The advantage of the method is that it can be used for any number of measurements in the network. SVM was used in [19] to identify the fault type, faulty section and distance together of faulted lines in a transmission system.

Most of the previous fault location methods diagnose faults for transmission systems but not in unbalanced distribution systems. Different from transmission systems, distribution systems have more complex topological structures with multiple laterals. The methods focus on finding the fault type or the fault distance separately. None of the researches presents effective fault location identification by considering the faulted phase, fault type, faulty section and fault distance at the same time in an unbalanced distribution system. Considering this limitation, this work tends to identify faulted phase, fault type, faulty section and fault distance in a single method. The fault type itself includes the faulted phase which are Single Line to Ground Fault at phase a ($SLGF_a$), Single Line to Ground Fault at phase b ($SLGF_b$), Single Line to Ground Fault at phase c ($SLGF_c$), Line to Line Fault at phase ab (LLF_{ab}), Line to Line Fault at phase bc (LLF_{bc}), Line to Line Fault at phase ca (LLF_{ca}), Double Line to Ground Fault at phase ab ($DLGF_{ab}$), Double Line to Ground Fault at phase bc ($DLGF_{bc}$), Double Line to Ground Fault at phase ca ($DLGF_{ca}$) and Three phase to ground fault at phase abc ($LLLGF_{abc}$).

The proposed method locates fault using three-dimensional (3D) analysis of SVM. The faulted phase and the fault type are identified using multiclass Support Vector Classification (SVC). The faulty section is identified by estimating fault resistance using Support Vector Regression (SVR). The possible sections are identified by matching the actual voltage sag with the simulated data and the most possible sections are ranked. Finally, the fault distance is estimated using SVR analysis. This manuscript is organized in 5 sections. Section 2 describes the proposed methodology of the work. Section 3 presents the test system and section 4 gives the test results of the proposed method. Section 5 concludes the finding of this work.

2. Proposed Methodology

The proposed method utilizes voltage sag magnitude for 3 phases (phase a, b and c) to identify the fault in unbalanced distribution systems. It first identifies the fault type including faulted phase, then the faulty section and finally the fault distance. The illustration of proposed method is shown in Figure 1.

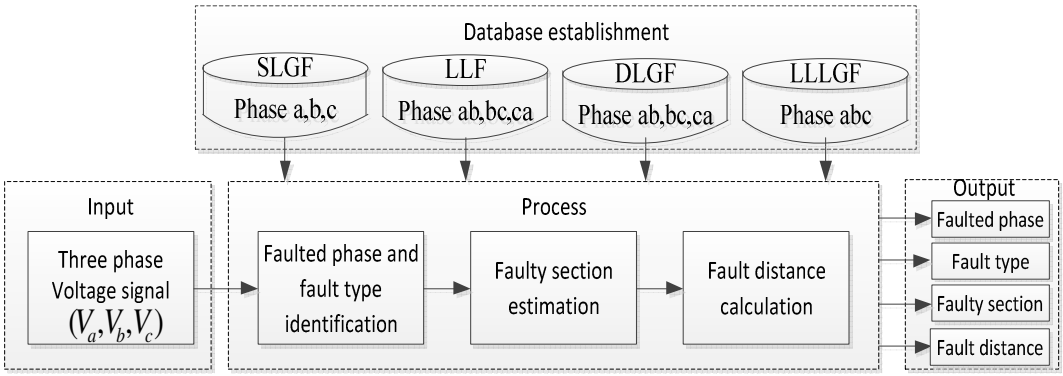

Figure 1: Illustration of the proposed method

2.1. Database establishment

The proposed method is implemented using SVM which requires a training set of voltage sag data for processing. The database establishment is illustrated in Figure 2. The steps involve are as follows:

1. Single Line to Ground Fault at phase a ($SLGF_a$) is simulated at all nodes of distribution system with 0Ω resistance
2. Voltage sag magnitude at phase a, b and c are recorded from the measurement node
3. The simulation is repeated for fault resistance of 20Ω, 40Ω and 60Ω resistance
4. Steps 1 to 3 are repeated for other fault types of $SLGF_b$, $SLGF_c$, LLF_{ab}, LLF_{bc}, LLF_{ca}, $DLGF_{ab}$, $DLGF_{bc}$, $DLGF_{ca}$ and $LLLGF_{abc}$.

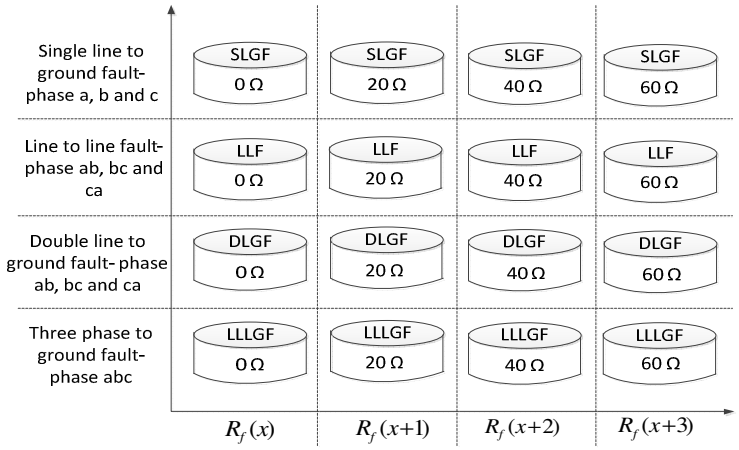

Figure 2: Training data establishment

2.2. Fault type identification

The type of fault can be identified using 'one versus all' concept of multiclass SVC. The proposed method uses voltage sag data at fault (V_{af}, V_{bf} and V_{cf}) as input for SVC. The desired output is the type of the fault. Figure 3 describes the fault type classification using SVC. At each SVC, there are two possible inputs for classification, class 1 and class 0. At first, the voltage sag data of $SLGF_a$ is considered as class 1 and the remaining ($SLGF_b$, $SLGF_c$, LLF_{ab}, LLF_{bc}, LLF_{ca}, $DLGF_{ab}$, $DLGF_{bc}$, $DLGF_{ca}$ and $LLLGF_{abc}$) are considered as class 0. SVC finds the optimal hyper-plane between the two classes and identifies whether the input data falls in class 1 or class 0. If the fault type is identified under class 1, then the fault type is finalized as $SLGF_a$. If the fault type is identified under class 0, then a second step of classification takes place by considering $SLGF_b$ as class 1 and the remaining ($SLGF_c$, LLF_{ab}, LLF_{bc}, LLF_{ca}, $DLGF_{ab}$, $DLGF_{bc}$, $DLGF_{ca}$ and $LLLGF_{abc}$) as class 0. The process is continued until the actual fault type is identified.

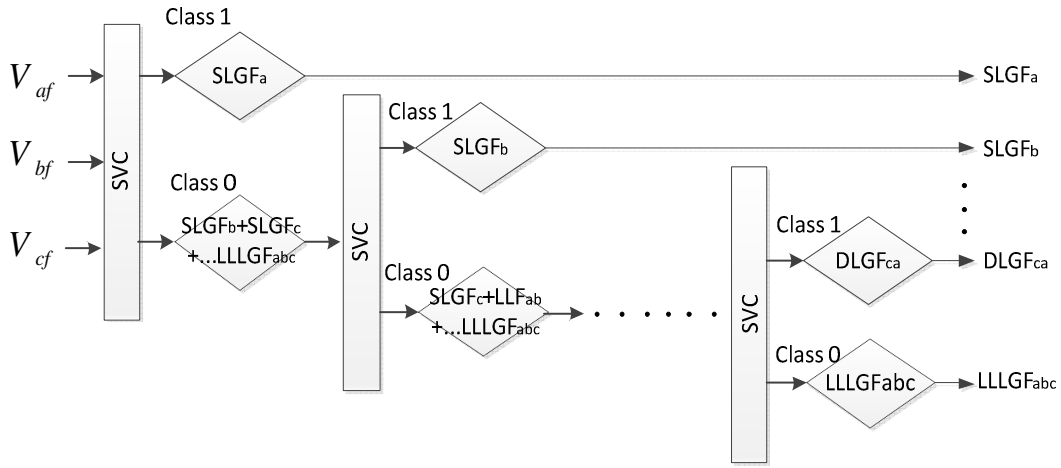

Figure 3: Fault type identification using SVC

2.3. Faulty section identification

Once the fault type is identified, the faulty section is identified. Faulty section identification consists of fault resistance estimation, selection of possible sections and ranking analysis.

2.3.1 Fault resistance estimation

Fault resistance is estimated using SVR analysis. The voltage sag data from database is trained using radial basis function in SVR. The voltage sag at fault conditions (V_{af}, V_{bf} and V_{cf}) are assigned as the input to SVR. The corresponding output (R_f^{est}) is the estimated fault resistance. The illustration of the fault resistance estimation is depicted in Figure 4.

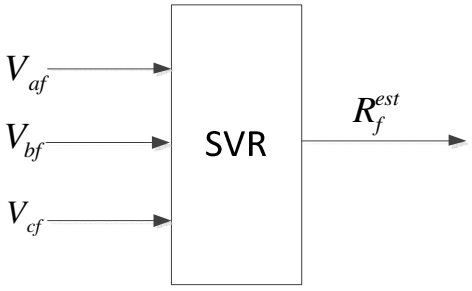

Figure 4: Fault resistance estimation using SVR

2.3.2 Selection of possible sections

Once the fault resistance is estimated, the possible faulty sections are identified by comparing the voltage sag magnitude in database with the actual voltage sag magnitude [17, 20]. The fault resistance from the database are selected such that,

$$R_f(x) < R_f^{est} < R_f(x+1) \quad (1)$$

where of $R_f(x)$ and $R_f(x+1)$ are the resistance from database for which the voltage sag is simulated.

The voltage sag data for each section from $R_f(x)$ and $R_f(x+1)$ are analysed individually. For example, a faulty section *s* between nodes *i* and *j* are considered. The voltage sag magnitudes with a fault resistance between $R_f(x)$ and $R_f(x+1)$ are shown in Table 1.

Table 1: Voltage sag data for section identification

Node	Fault resistance in database	
	$R_f(x)$	$R_f(x+1)$
Node *i*	$V_{a,i}^{R_f(x)}, V_{b,i}^{R_f(x)}, V_{c,i}^{R_f(x)}$	$V_{a,i}^{R_f(x+1)}, V_{b,i}^{R_f(x+1)}, V_{c,i}^{R_f(x+1)}$
Node *j*	$V_{a,j}^{R_f(x)}, V_{b,j}^{R_f(x)}, V_{c,j}^{R_f(x)}$	$V_{a,j}^{R_f(x+1)}, V_{b,j}^{R_f(x+1)}, V_{c,j}^{R_f(x+1)}$

Figure 5 showsthe search boundary of section *s* at resistance values, $R_f(x)$ and $R_f(x+1)$ in 3D. (V_{af}, V_{bf}, V_{cf}) correspondingto the measured voltage sag magnitude at phase a, b and c at fault condition. It can be seen that the measured voltage sag is not within the search boundary. To address this problem, the minimum and maximum voltage sag profiles of two adjacent fault resistances are considered.

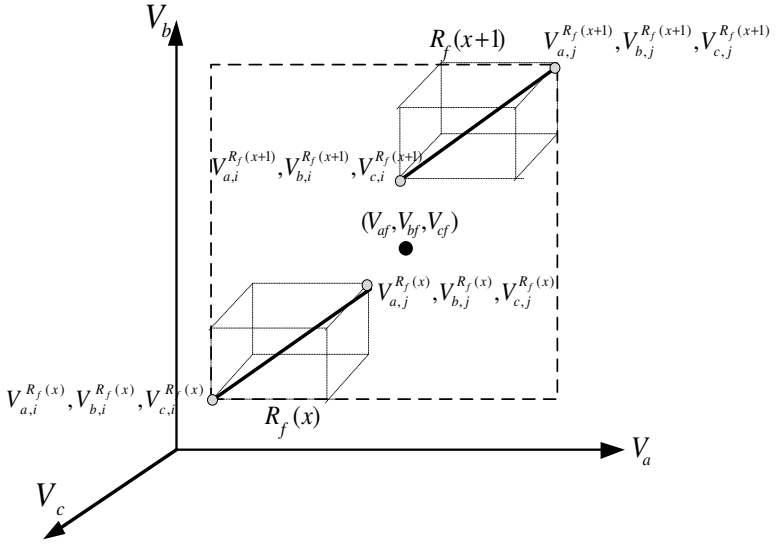

Figure 5: Voltage sag profile variation for section *s* and two different resistances

The minimum and maximum voltage sags of the section *s* are noted down. If the voltage sag at fault lies between minimum and maximum of the section from database, the corresponding section is chosen as the faulty section [17].

$$V_{a,i}^{R_f(x)} \le V_{af} \le V_{a,j}^{R_f(x+1)} \quad (2)$$

$$V_{b,i}^{R_f(x)} \le V_{bf} \le V_{b,j}^{R_f(x+1)} \quad (3)$$

$$V_{c,i}^{R_f(x)} \le V_{cf} \le V_{c,j}^{R_f(x+1)} \quad (4)$$

2.3.3 Ranking Analysis

Multiple faulty sections are possible in distribution system due to the presence of lateral branches and sub-branches. Hence the most possible faulty section is ranked using the similar concept of shortest distance principle [18]. The shortest distance d_s is calculated between the fault point and the linear line joining voltage sag from database. The faulty section, which yields the shortest distance among all possible faulty section has a high priority of the most possible faulty section. Figure 6 shows two possible faulty sections *s* (nodes *i-j*) and *m*(nodes *p-q*). $V_{a,i}^{R_f(x)}, V_{b,i}^{R_f(x)}, V_{c,i}^{R_f(x)}$ and $V_{a,j}^{R_f(x+1)}, V_{b,j}^{R_f(x+1)}, V_{c,j}^{R_f(x+1)}$ represent the minimum and maximum values of voltage sag at section *s*. $V_{a,p}^{R_f(x)}, V_{b,p}^{R_f(x)}, V_{c,p}^{R_f(x)}$ and $V_{a,q}^{R_f(x+1)}, V_{b,q}^{R_f(x+1)}, V_{c,q}^{R_f(x+1)}$ represent the minimum and maximum values of voltage sag at section *m*. (V_{af}, V_{bf}, V_{cf}) represents the voltage sag data identified during the fault. d_{s1} and d_{s2} represent the shortest distance between the fault point and the line joining minimum and maximum values of sections *s* and *m*.

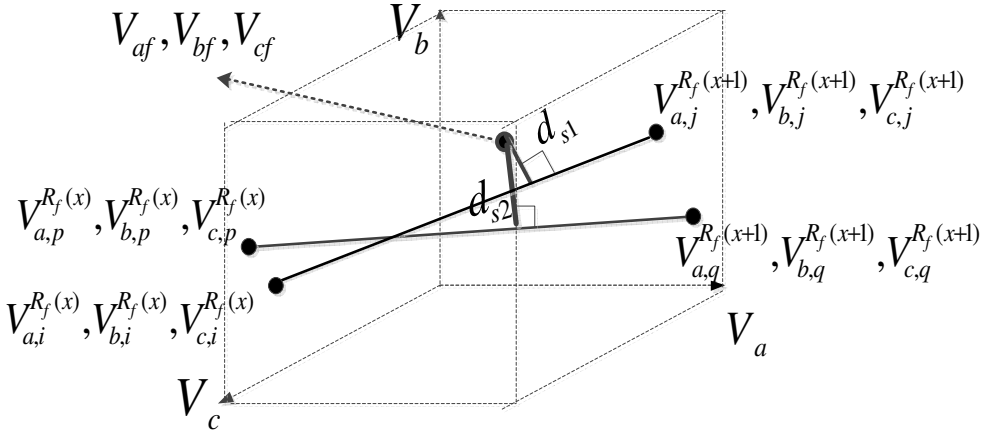

Figure 6: Ranking analysis

The shortest distance d_{s1} for a section *s* is calculated using

$$d_{s1} = \frac{|\bar{M}|}{|\bar{S}|} = \frac{\sqrt{M_x^2 + M_y^2 + M_z^2}}{\sqrt{S_x^2 + S_y^2 + S_z^2}} \quad (5)$$

where $\overline{S} = \{S_x, S_y, S_z\}$ is the directing vector of line joining $V_{a,i}^{R_f(x)}, V_{b,i}^{R_f(x)}, V_{c,i}^{R_f(x)}$ and $V_{a,j}^{R_f(x+1)}, V_{b,j}^{R_f(x+1)}, V_{c,j}^{R_f(x+1)}$

$\overline{N} = \{N_x, N_y, N_z\}$ is the directing vector of line joining $V_{a,i}^{R_f(x)}, V_{b,i}^{R_f(x)}, V_{c,i}^{R_f(x)}$ and (V_{af}, V_{bf}, V_{cf})

$\overline{M} = \{M_x, M_y, M_z\}$ is the cross product of vectors $\overline{N}$ and $\overline{S}$.

2.4. Fault Distance estimation

Fault distance is identified using SVR analysis. For the possible faulty sections, the voltage sag data at nodes from the database (Table 1) is trained using SVR to estimate the fault distance. The training input and output for section *s* is shown in Table 2. Here, l represents the length of the line section.

Table 2: Training data for fault distance calculation

Input training data	Output training data
$V_{a,i}^{R_f(x)}, V_{b,i}^{R_f(x)}, V_{c,i}^{R_f(x)}$	0
$V_{a,i}^{R_f(x+1)}, V_{b,i}^{R_f(x+1)}, V_{c,i}^{R_f(x+1)}$	0
$V_{a,j}^{R_f(x)}, V_{b,j}^{R_f(x)}, V_{c,j}^{R_f(x)}$	l
$V_{a,j}^{R_f(x+1)}, V_{b,j}^{R_f(x+1)}, V_{c,j}^{R_f(x+1)}$	l

The illustration for fault distance estimation is shown in Figure 7. The voltage sag data during the fault (V_{af}, V_{bf}, V_{cf}) and the estimated fault resistance R_f^{est} are assigned as input to SVR. The corresponding output is the fault distance f_d.

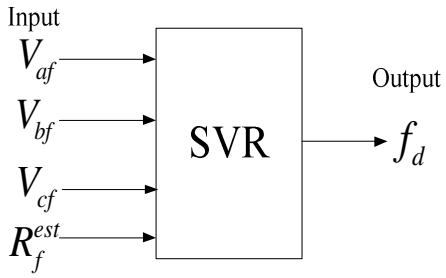

Figure 7: Fault distance estimation

3. Test System

The SaskPower network is a radial distribution network consisting of unbalanced lines and unbalanced loads. The schematic diagram of test distribution system is shown in Figure 8. The system consists of a 25kV equivalent source, single phase laterals, three phase

laterals and 20 line sections made up of different conductor. A node number is indicated along the line of the test system. The parameters of equivalent source, line data and the load data can be obtained from [17, 21, 22].

The distribution system is modelled using PSCAD power system simulation software. The cables are modelled as constant impedance load using PI model. The voltage sag data is recorded in measurement node nearer to node 1 of distribution system. The voltage sag database is created by simulating fault at all nodes of the distribution system. The performance of algorithm is tested for various fault types such as $SLGF_a$, $SLGF_b$, $SLGF_c$, LLF_{ab}, LLF_{bc}, LLF_{ca}, $DLGF_{ab}$, $DLGF_{bc}$, $DLGF_{ca}$ and $LLLGF_{abc}$ and for various resistances of 0Ω, 10Ω, 30Ω and 50Ω. The measured voltage sag data at the fault is analysed using a MATLAB programming code.

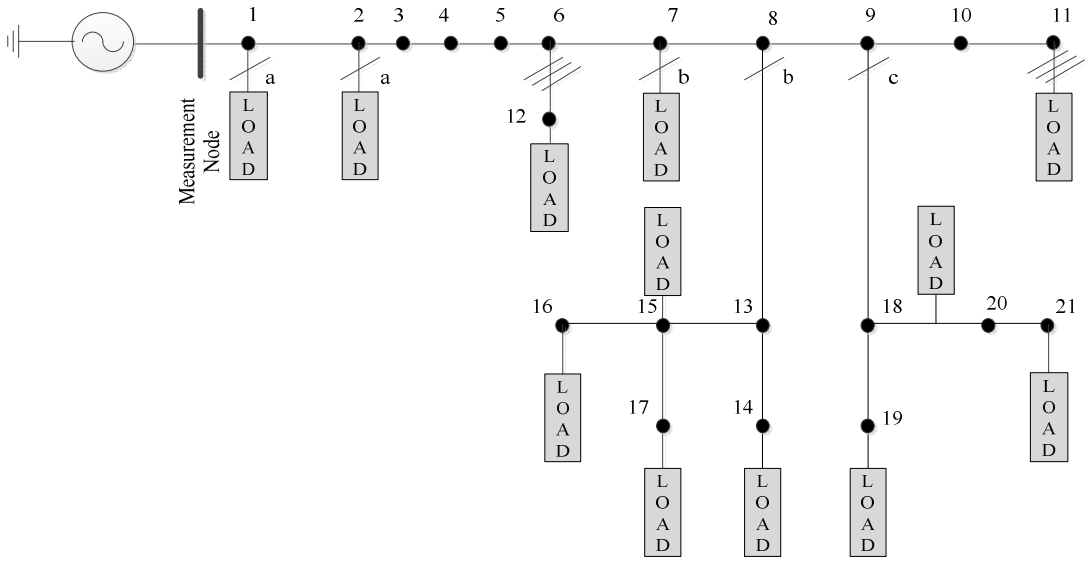

Figure 8: Schematic diagram of SaskPower Distribution system

4. Test Results

For training purpose, simulations were performed for fault at the nodes of the distribution system at 0Ω, 20Ω, 40Ω and 60Ω resistance. A total of 840*3 voltage sag data are utilized for training using SVM. For testing purpose, faults at the middle of the line section at 0Ω, 10Ω, 30Ω and 50Ω resistance.

4.1. Fault type classification

The proposed method is tested for ten fault types ($SLGF_a$, $SLGF_b$, $SLGF_c$, LLF_{ab}, LLF_{bc}, LLF_{ca}, $DLGF_{ab}$, $DLGF_{bc}$, $DLGF_{ca}$ and $LLLGF_{abc}$). The subscript in the fault type represents the faulted phase. The fault type and the faulted phase are identified using 3D multiclass SVC. SVC is trained with 840 voltage samples using radial basis function (RBF) for classification of 10 output. The support vectors identified using SVC during fault type classification are tabulated in Table 3.

Table 3: Support vectors of SVC

Types of fault	Class 1	Class 0	Identified Support vectors
$SLGF_a$	84	756	144
$SLGF_b$	84	672	137
$SLGF_c$	84	588	128
LLF_{ab}	84	504	82
LLF_{bc}	84	420	81
LLF_{ca}	84	336	80
$DLGF_{ab}$	84	252	56
$DLGF_{bc}$	84	168	49
$DLGF_{ca}$ and $LLLGF_{abc}$	84	84	43

The hyper plane obtained for fault type classification is shown in Figure 9(a) to Figure 9(i). Figure 9(a) gives the total of 840 voltage sag data and 3D non-linear hyperplane identified for $SLGF_a$. Class 1 represents the data of $SLGF_a$ and the remaining ($SLGF_b$, $SLGF_c$, LLF_{ab}, LLF_{bc}, LLF_{ca}, $DLGF_{ab}$, $DLGF_{bc}$, $DLGF_{ca}$ and $LLLGF_{abc}$) as Class 0. The x-axis represents the voltage at phase a, y-axis represents the voltage at phase b and z-axis represents the voltage at phase c. If the fault type is not $SLGF_a$ then further classification is carried out by considering $SLGF_b$ as class 1 as given in Figure 9(b). Similarly the hyperplane for classification of fault types $SLGF_c$, LLF_{ab}, LLF_{bc}, LLF_{ca}, $DLGF_{ab}$, $DLGF_{bc}$, $DLGF_{ca}$ and $LLLGF_{abc}$ are shown in Figure 9(c) to Figure 9(i)

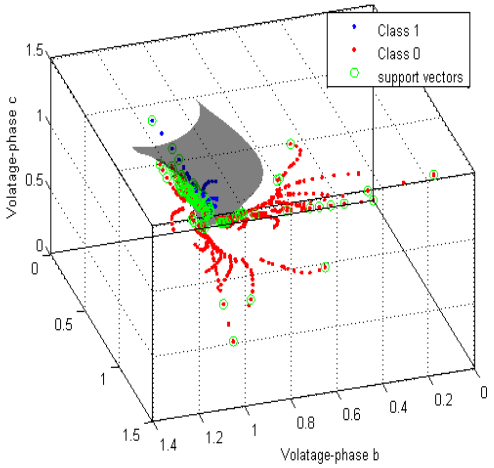

9(a) 3D hyper plane for $SLGF_a$

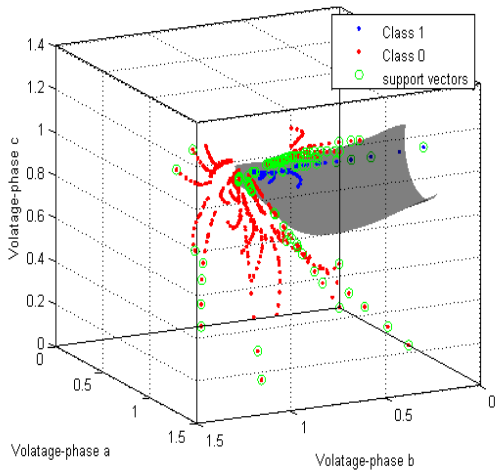

9(b) 3D hyper plane for $SLGF_b$

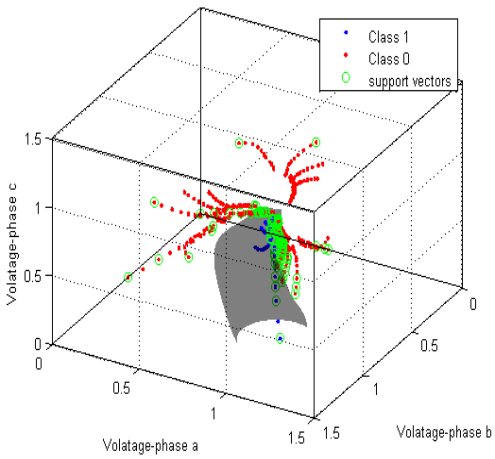

9(c) 3D hyper plane for $SLGF_c$

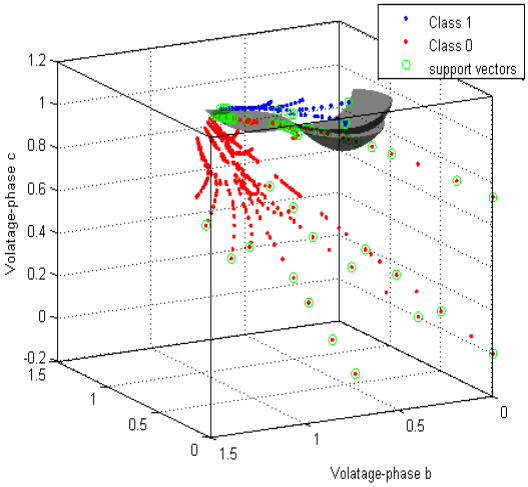

9(d) 3D hyper plane for LLF_{ab}

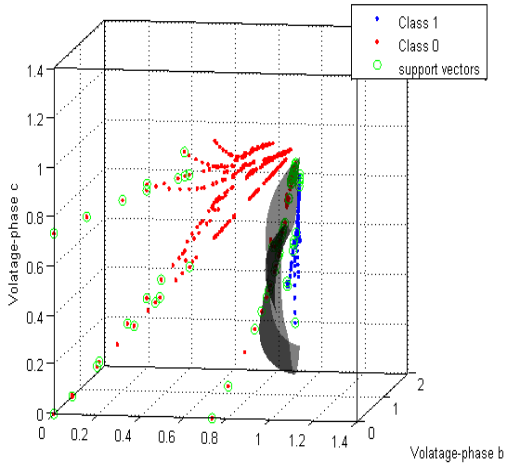

9(e) 3D hyper plane for LLF_{bc}

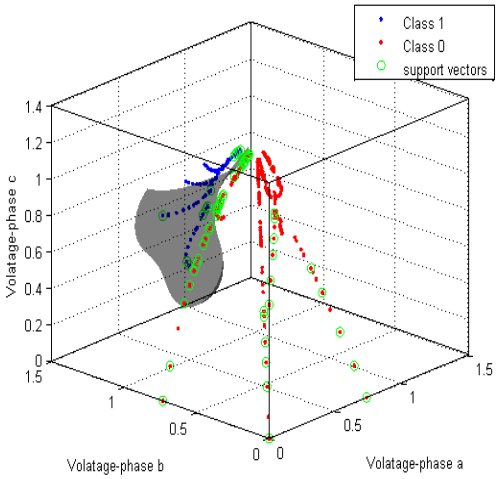

9(f) 3D hyper plane for LLF_{ca}

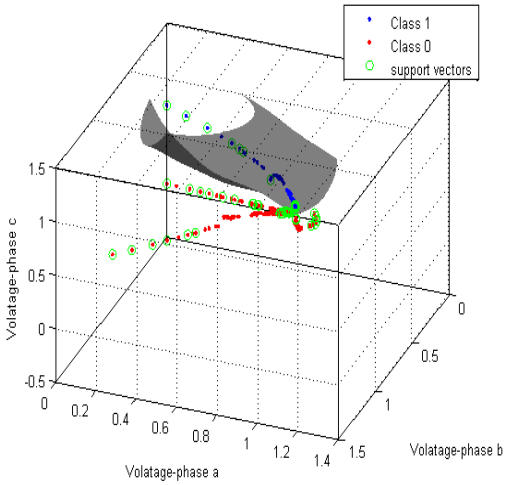

9(g) 3D hyper plane for $DLGF_{ab}$

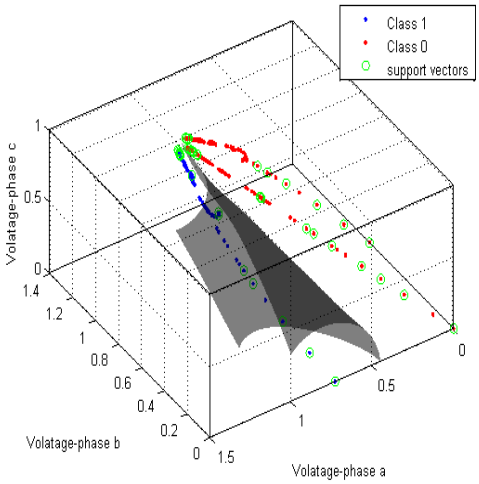

9(h) 3D hyper plane for $DLGF_{bc}$

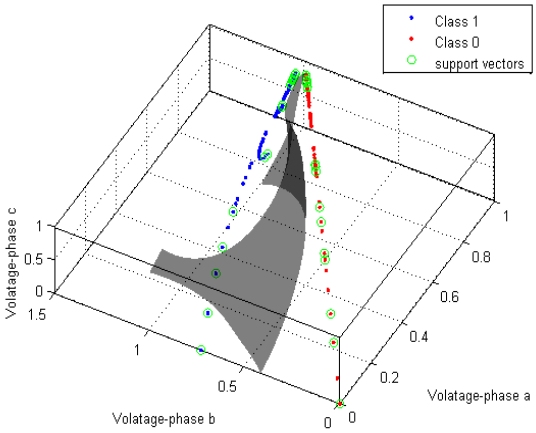

9(i) 3D hyper plane for $DLGF_{ca}$ and $LLLGF_{abc}$

Figure 9: 3D classification using SVC

4.2. Faulty section

The test results of possible faulty sections and rank of the correct section at 0Ω resistance is illustrated in Table 4. For analysis, the test sections 1-2 and 7-8 nodes (Main at feeder), 13-14 nodes (Branch at feeder), 18-20 nodes (Sub branch at feeder) are considered. From the results, it can be noted that single faulty sections were selected for test sections 1-2 and 7-8 for all types of fault. This is because, from node 1 to node 2 and node 7 to node 8 is completely a radial line and there are no parallel line sections. Also the rank identified for the fault type of $SLGF_a$, $SLGF_b$ and $SLGF_c$; LLF_{ab}, LLF_{bc} and LLF_{ca}; $DLGF_{ab}$, $DLGF_{bc}$ and $DLGF_{ca}$ are the same. This is due to only the faulted phase is interchanged.

Table 4: Faulty sections and rank of the correct section at0Ω resistance

Section Number	Test Section	Selected Faulty Section	Rank Number of the Actual Faulty Section			
			$SLGF_a$/ $SLGF_b$/ $SLGF_c$	LLF_{ab}/ LLF_{bc}/ LLF_{ca}	$DLGF_{ab}$/ $DLGF_{bc}$/ $DLGF_{ca}$	$LLLGF_{abc}$
1	1-2	1-2	1	1	1	1
7	7-8	7-8	1	1	1	1
13	13-14	13-14, 13-15, 18-19, 18-20	1	1	1	1
19	18-20	13-14, 13-15, 18-19, 18-20	2	3	3	2

The test results of faulty section are also analysed for various other fault resistances of 10Ω, 30Ω and 50Ω. The calculated fault resistance and the ranking using shortest distance principle for test section 1-2, 7-8, 13-14 and 18-20 nodes are tabulated in Table 5. It can be noted that the calculated fault resistance is closer to the actual resistance.

Table 5: Fault resistance and ranking of the faulty sections

Faulty section	Actual fault resistance	$SLGF_a$, $SLGF_b$, $SLGF_c$		LLF_{ab}, LLF_{bc}, LLF_{ca}		$DLGF_{ab}$, $DLGF_{bc}$, $DLGF_{ca}$		$LLLGF_{abc}$	
		Calculated resistance (Ω)	Rank	Calculated resistance (Ω)	Rank	Calculated resistance (Ω)	Rank	Calculated resistance (Ω)	Rank
1-2	10	10.487	1	13.399	1	9.152	1	10.983	1
	30	30.386	1	31.767	1	28.044	2	27.782	1
	50	51.875	1	52.799	1	50.802	1	47.828	1
7-8	10	11.629	2	9.0094	1	11.579	2	11.959	1
	30	29.362	1	32.011	2	28.277	4	28.040	1
	50	53.888	3	50.617	3	46.724	1	48.456	2
13-14	10	11.269	1	13.571	2	9.038	1	11.272	3
	30	29.683	3	30.791	5	32.550	4	33.701	2
	50	46.712	3	49.886	6	48.093	2	51.218	2
18-20	10	12.085	1	13.581	2	9.970	4	12.751	2
	30	30.073	1	27.074	1	29.684	1	28.390	4
	50	48.904	5	48.820	2	49.694	4	51.566	1

The overall ranking performance of the proposed method is shown in Figure 10. The x-axis represents the rank and y-axis represents the number of possible candidate identified in the ranking. The test cases are repeated for resistances of 0Ω, 10Ω, 30Ω and 50Ω for fault at the midpoint of all 20 line sections. It shows that most of the possible faulty sections are found correctly at the first and second ranks for mid-point tests at all test sections. For 0Ω resistance, 14 faulty sections are correctly identified in the first rank for LLF, 15 sections for SLGF and DLGF and 18 sections for LLLGF. The faulty section performances of LLF (2 sections) and DLGF (1 section) have rankings, up to the third rank. For other fault resistances of 10Ω, 30Ω and 50Ω, the result shows that all of the sections can be determined within first six ranks.

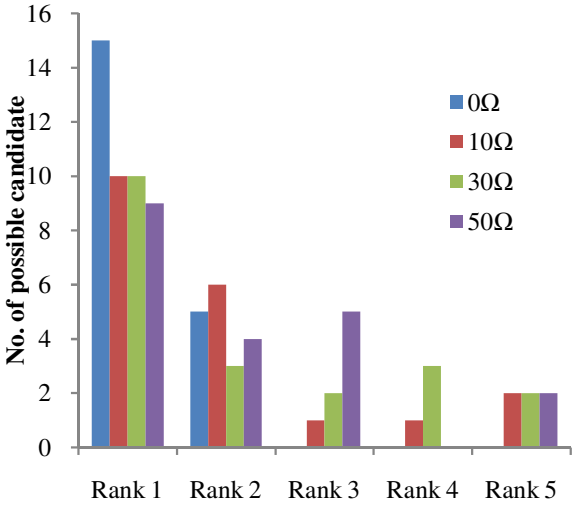

10(a) $SLGF_a$, $SLGF_b$, $SLGF_c$

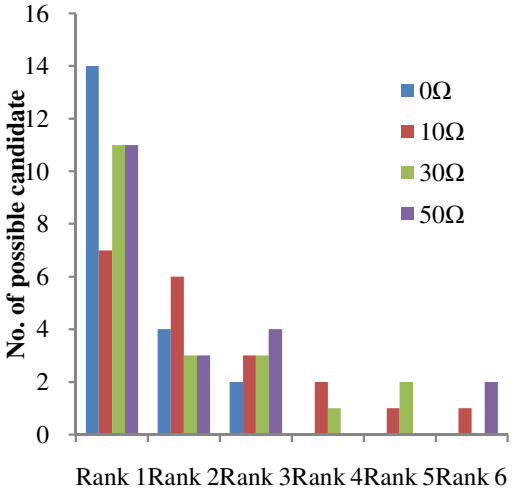

10(b) LLF_{ab}, LLF_{bc}, LLF_{ca}

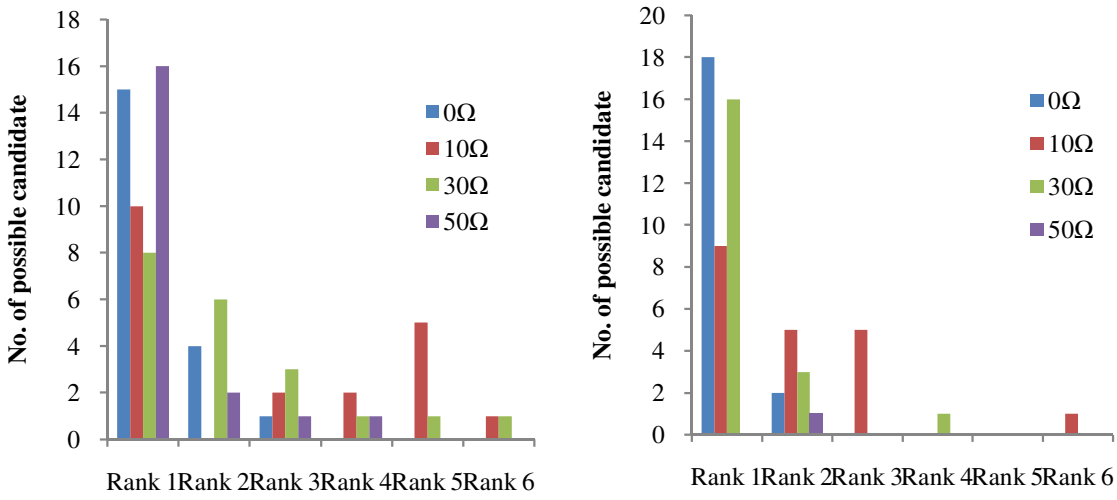

10(c) $DLGF_{ab}$, $DLGF_{bc}$, $DLGF_{ca}$ 10(d) $LLLGF_{abc}$

Figure 10: Overall ranking performance

4.3. Fault distance calculation

The fault distance isanalysed using SaskPower distribution network for fault at the midpoint of all line section. Figure 11 shows the percentage error of calculated fault distance for SLGFat resistances of 0Ω, 10Ω, 30Ω and 50Ω. The test results of fault distance for $SLGF_a$, $SLGF_b$ and $SLGF_c$ are the same because the voltage sag at phase a, phase b and phase c are just interchanged. A maximum percentageerror of 24.7% isobtained in SLGF (section 1-2)at a faultresistance of 10Ω.

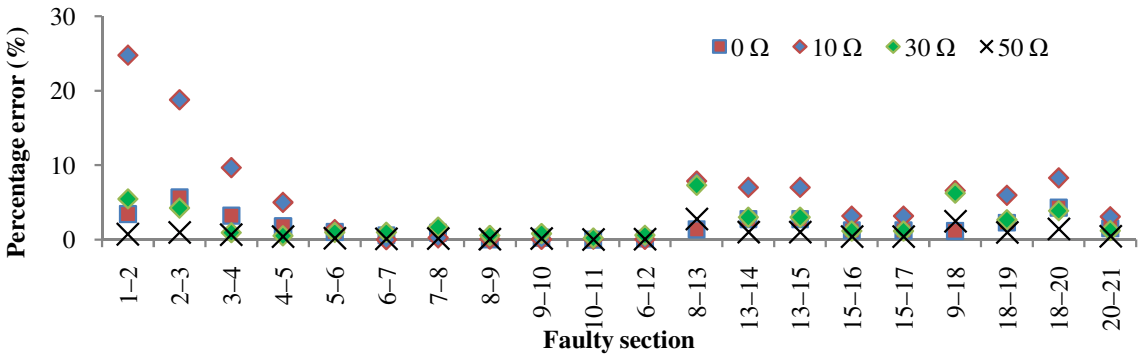

Figure 11: Calculated fault distance for $SLGF_a$/ $SLGF_b$/ $SLGF_c$

The percentageerror for LLF_{ab}, LLF_{bc} and LLF_{ca}at resistances of 0Ω, 10Ω, 30Ω and 50Ωisshown in Figure 12. A maximum percentageerror of 11.3% isobtained in test section 1-2 at10Ωresistance. All other test sections havelowerpercentageerror.

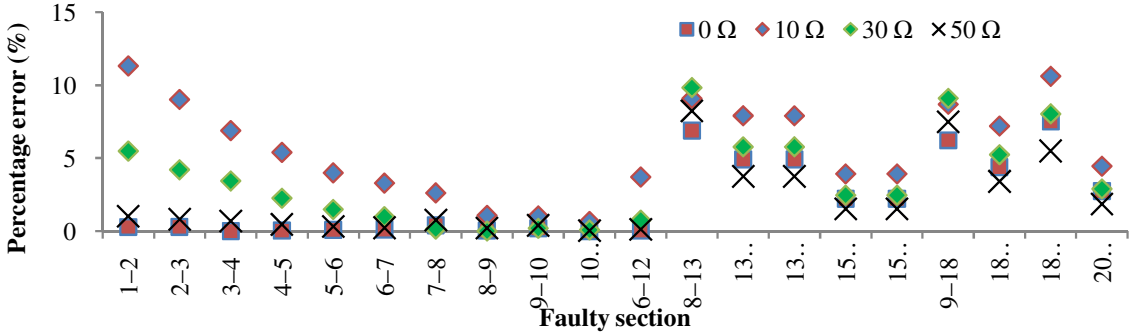

Figure 12: Calculated fault distance for LLF_{ab}/ LLF_{bc}/ LLF_{ca}

The percentageerror of fault distance for $DLGF_{ab}$, $DLGF_{bc}$ and $DLGF_{ca}$at resistances of 0Ω, 10Ω, 30Ω and 50Ωisshown in Figure 13. A maximum of 23% isidentified in test section 1-2 at 10Ω resistance.

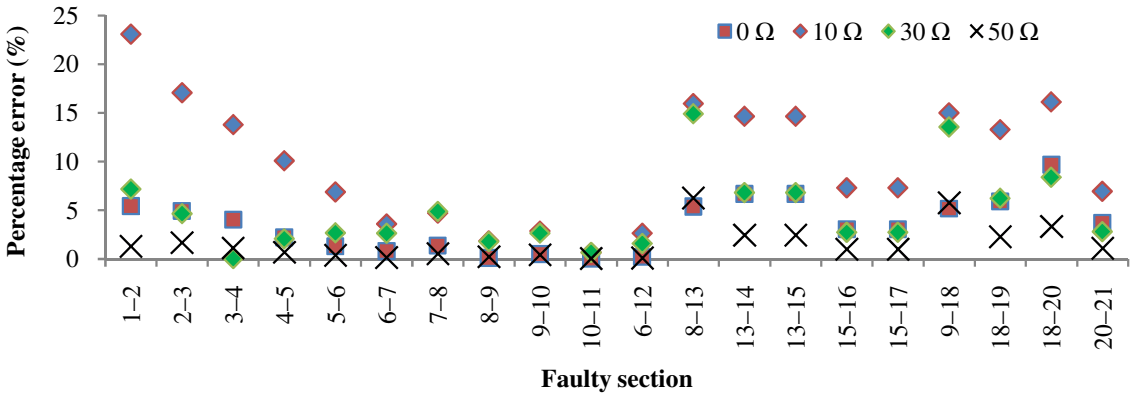

Figure 13: Calculated fault distance for $DLGF_{ab}$/ $DLGF_{bc}$/ $DLGF_{ca}$

Figure 14 gives the percentage error of $LLLGF_{abc}$ .A maximum percentage error of 30% is obtained at 10 Ω resistance (at section 1-2) for $LLLGF_{abc}$. In this, the deviation from the actual fault distance is 362 meters which is a small distance compared to the whole distribution system. The percentage error of fault distance at other resistance of 0 Ω, 30 Ω and 50 Ω are less than 30% error. Therefore, the proposed method has managed to identify the fault distance with greater accuracy.

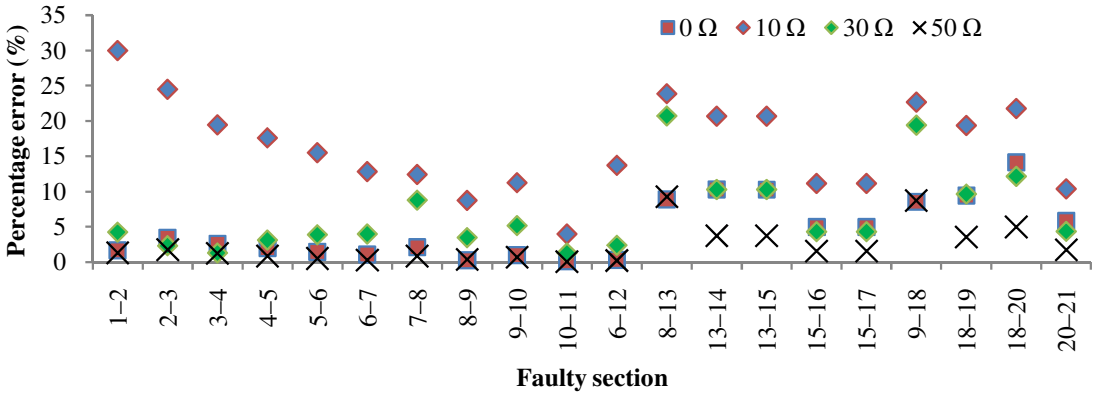

Figure 14: Calculated fault distance for $LLLGF_{abc}$

5. Conclusions

An approach using three-dimensional support vector classification and regression analysis for locating fault has been successfully proposed in this work. The fault type and the faulted phase are identified using SVC. The method classifies all 10 types of faults by identifying the hyper plane between classes. The faulty section was identified by using matching approach and ranking the most possible faulty section. The possible faulty section was ranked using three-dimensional shortest distance principle. The proposed work shows that the faulty sections were identified within first six ranking and all of the faulty sections can be ranked. Also, fault distances for the possible faulty sections were identified using SVR analysis. A maximum error of 30% was obtained in the test cases. Therefore, the proposed method has the potential to be used to identify the faulted phase, fault type, faulty section and fault distance for various fault resistances.

Acknowledgement

The authors thank the Malaysian Ministry of Education and University of Malaya for supporting this work through research grant of HIR (H-16001-D00048) and FRGS (FP026-2012A).

References

[1] U.-C. P. S. O. T. Force, Abraham, S., et al. , US-Canada Power System Outage Task Force, *Final Report on the August 14, 2003 Blackout in the United States and Canada: Causes and Recommendations,* 2004.

[2] Y. Menchafou, M. Zahri, M. Habibi, and H. E. Markhi, Extension of the Accurate Voltage-Sag Fault Location Method in Electrical Power Distribution Systems,*Journal of Electrical Systems,* 12, 33-44, 2016.

[3] M. R. Garousi, M. R. Shakarami, and F. Namdari, Detection and classification of power quality disturbances using parallel neural networks based on discrete wavelet transform, *Journal of Electrical Systems,* 12, 158-173, 2016.

[4] C. T. Suresh Kamble, Voltage Sag Characterization in a Distribution Systems: A Case Study, *Journal of Power and Energy Engineering,* 2, 546-553, 2014.

[5] D. M. K. Namrata B. Pawar, Generation of Different Types of Voltage Sag Using Matlab/Simulink, *International Journal of Engineering and Innovative Technology,* 3, 2014.

[6] A. K. Pradhan, A. Routray, and B. Biswal, Higher order statistics-fuzzy integrated scheme for fault classification of a series-compensated transmission line,*IEEE Transactions on Power Delivery,* 19, 891-893, 2004.

[7] B. Das and J. V. Reddy, Fuzzy-logic-based fault classification scheme for digital distance protection,*IEEE Transactions on Power Delivery,* 20, 609-616, 2005.

[8] B. Das, Fuzzy logic-based fault-type identification in unbalanced radial power distribution system,*IEEE Transactions on Power Delivery,* 21, 278-285, 2006.

[9] A. Flores, E. Quiles, E. García, and F. Morant, Novel Formulation using Artificial Neural Networks for Fault Diagnosis in Electric Power Systems – A Modular Approach,*Journal of Electrical Systems,* 6, 2010.

[10] U. B. Parikh, B. Das, and R. Maheshwari, Fault classification technique for series compensated transmission line using support vector machine, *International Journal of Electrical Power & Energy Systems,* 32(7), 629-636, 2010.

[11] Y. Guo, K. Li, and X. Liu, Fault Diagnosis for Power System Transmission Line Based on PCA and SVMs,*Intelligent Computing for Sustainable Energy and Environment*, 355, 524-532, 2013.

[12] P. K. Dash, S. R. Samantaray, and G. Panda, Fault Classification and Section Identification of an Advanced Series-Compensated Transmission Line Using Support Vector Machine, *IEEE Transactions on Power Delivery,* 22, 67-73, 2007.

[13] A. J. Prarthana Warlyani, A.S.Thoke, and R.N.Patel, Fault Classification and Faulty Section Identification in Teed Transmission Circuits Using ANN,*International Journal of Computer and Electrical Engineering,*3, 807-811, 2011.

[14] S. Ekici, Support Vector Machines for classification and locating faults on transmission lines,*Applied Soft Computing,* 12(6), 1650-1658,2012.

[15] P. Ray, B. K. Panigrahi, and N. Senroy, Hybrid methodology for fault distance estimation in series compensated transmission line,*IET Generation, Transmission & Distribution,* 7, 431-439, 2013.

[16] A. Saber, A. Emam, and R. Amer, Discrete wavelet transform and support vector machine-based parallel transmission line faults classification, *IEEJ Transactions on Electrical and Electronic Engineering,* 2015.

[17] H. Mokhlis and H. Li, Non-linear representation of voltage sag profiles for fault location in distribution networks,*Electrical Power and Energy Systems,* 33, 124–130, 2011.

[18] L. J. Awalin, H. Mokhlis, A. Abu Bakar, H. Mohamad, and H. A. Illias, A generalized fault location method based on voltage sags for distribution network,*IEEJ Transactions on Electrical and Electronic Engineering,* 8, S38-S46, 2013.

[19] B. Ravikumar, D. Thukaram, and H. P. Khincha, Application of support vector machines for fault diagnosis in power transmission system,*IET Generation, Transmission & Distribution,* 2, 119-130, 2008.

[20] L. H. Mokhlis H, Khalid AR., The application of voltage sags pattern to locate a faulted section in distribution network, *IEEE International Review of Electrical Engineering,* 5, 173–179, 2010.

[21] J. Mora-Flòrez, J. Meléndez, and G. Carrillo-Caicedo, Comparison of impedance based fault location methods for power distribution systems, *Electric Power Systems Research,* 78(4), 657-666, 2008.

[22] L. Seung-Jae, C. Myeon-Song, K. Sang-Hee, J. Bo-Gun, L. Duck-Su, A. Bok-Shin*, et al.*, An intelligent and efficient fault location and diagnosis scheme for radial distribution systems, *IEEE Transactions on Power Delivery,* 19, 524-532, 2004.